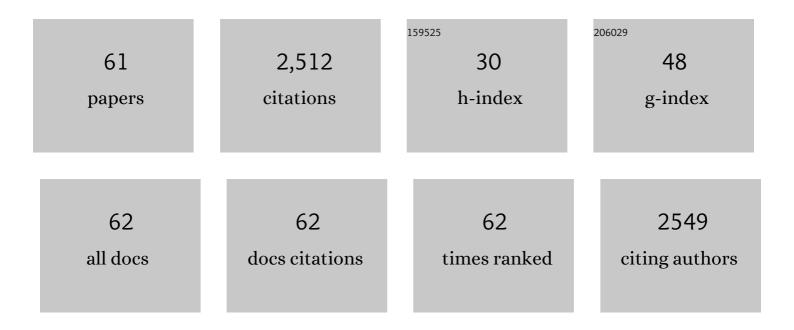
List of Publications by Year in descending order

Source: https://exaly.com/author-pdf/18494/publications.pdf Version: 2024-02-01



#	Article	IF	CITATIONS
1	Ru-functionalized Ni-doped dual phases of α/γ-Fe2O3 nanosheets for an optimized acetone detection. Journal of Nanostructure in Chemistry, 2023, 13, 577-589.	5.3	4
2	Enhanced microwave absorption of biomass carbon/nickel/polypyrrole (C/Ni/PPy) ternary composites through the synergistic effects. Journal of Alloys and Compounds, 2022, 890, 161887.	2.8	42
3	Magnetic FeOX/biomass carbon composites with broadband microwave absorption properties. Journal of Alloys and Compounds, 2022, 903, 163894.	2.8	31
4	MOF-on-MOF nanoarchitecturing of Fe2O3@ZnFe2O4 radial-heterospindles towards multifaceted superiorities for acetone detection. Chemical Engineering Journal, 2022, 442, 136094.	6.6	31
5	Ternary MXene/MnO2/Ni composites for excellent electromagnetic absorption with tunable effective absorption bandwidth. Journal of Alloys and Compounds, 2022, 911, 165122.	2.8	12
6	Effective fabrication of flexible nickel chains/acrylate composite pressure-sensitive adhesives with layered structure for tunable electromagnetic interference shielding. Advanced Composites and Hybrid Materials, 2022, 5, 2906-2920.	9.9	61
7	Ni Doping in MnO ₂ /MXene (Ti ₃ C ₂ T _{<i>x</i>}) Composites to Modulate the Oxygen Vacancies for Boosting Microwave Absorption. ACS Applied Electronic Materials, 2022, 4, 3694-3706.	2.0	13
8	Biomass derived porous carbon (BPC) and their composites as lightweight and efficient microwave absorption materials. Composites Part B: Engineering, 2021, 207, 108562.	5.9	177
9	Absorption-dominant radio-wave attenuation loss of metals and graphite. Journal of Materials Science, 2021, 56, 8037-8047.	1.7	16
10	1D Zn2GeO4 rods supported on Ni foam for high performance non-enzymatic hydrogen peroxide sensor. Surfaces and Interfaces, 2021, 25, 101295.	1.5	3
11	Radio-wave electrical conductivity and absorption-dominant interaction with radio wave of exfoliated-graphite-based flexible graphite, with relevance to electromagnetic shielding and antennas. Carbon, 2020, 157, 549-562.	5.4	48
12	Construction of natural fiber/polyaniline core-shell heterostructures with tunable and excellent electromagnetic shielding capability via a facile secondary doping strategy. Composites Part A: Applied Science and Manufacturing, 2020, 137, 105994.	3.8	69
13	NiO nanosheets on pine pollen-derived porous carbon: construction of interface to enhance microwave absorption. Journal of Materials Science: Materials in Electronics, 2020, , 1.	1.1	6
14	ZnO-Decorated In/Ga Oxide Nanotubes Derived from Bimetallic In/Ga MOFs for Fast Acetone Detection with High Sensitivity and Selectivity. ACS Applied Materials & Interfaces, 2020, 12, 26161-26169.	4.0	54
15	Tuning the microwave absorption capacity of TiP2O7 by composited with biomass carbon. Applied Surface Science, 2020, 515, 145974.	3.1	59
16	A nickel foam modified with electrodeposited cobalt and phosphor for amperometric determination of dopamine. Mikrochimica Acta, 2019, 186, 602.	2.5	6
17	MOFs-Derived Porous NiFe2O4 Nano-Octahedrons with Hollow Interiors for an Excellent Toluene Gas Sensor. Nanomaterials, 2019, 9, 1059.	1.9	25
18	Effect of the planar coil and linear arrangements of continuous carbon fiber tow on the electromagnetic interference shielding effectiveness, with comparison of carbon fibers with and without nickel coating. Carbon, 2019, 152, 898-908.	5.4	43

#	Article	IF	CITATIONS
19	Jute-based porous biomass carbon composited by Fe3O4 nanoparticles as an excellent microwave absorber. Journal of Alloys and Compounds, 2019, 803, 1119-1126.	2.8	51
20	Highly Sensitive and Selective Toluene Sensor of Bimetallic Ni/Fe-MOFs Derived Porous NiFe ₂ O ₄ Nanorods. Industrial & Engineering Chemistry Research, 2019, 58, 9450-9457.	1.8	27
21	In situ fabrication of Ni(OH)2 nanoflakes/K-Ti-O nanowires on NiTi foil for high performance non-enzymatic hydrogen peroxide sensing. Journal of Electroanalytical Chemistry, 2019, 842, 107-114.	1.9	5
22	Biomass carbon derived from pine nut shells decorated with NiO nanoflakes for enhanced microwave absorption properties. RSC Advances, 2019, 9, 9126-9135.	1.7	73
23	Preparation and electromagnetic shielding effectiveness of cobalt ferrite nanoparticles/carbon nanotubes composites. Nanomaterials and Nanotechnology, 2019, 9, 184798041983782.	1.2	26
24	In situ fabrication of Co(OH)2 by hydrothermal treating Co foil in MOH (M = H, Li, Na, K) for non-enzymatic glucose detection. Journal of Alloys and Compounds, 2019, 781, 1033-1039.	2.8	11
25	MOFs-derived NiFe2O4 fusiformis with highly selective response to xylene. Journal of Alloys and Compounds, 2019, 784, 102-110.	2.8	40
26	Fe3O4/Fe/C composites prepared by a facile thermal decomposition method and their application as microwave absorbers. Journal of Alloys and Compounds, 2019, 784, 1123-1129.	2.8	30
27	Microwave absorption performance of Ni(OH)2 decorating biomass carbon composites from Jackfruit peel. Applied Surface Science, 2018, 447, 261-268.	3.1	89
28	Synthesis of core-shell carbon sphere@nickel oxide composites and their application for supercapacitors. Ionics, 2018, 24, 513-521.	1.2	19
29	Highly sensitive nonenzymatic H2O2 sensor based on NiFe-layered double hydroxides nanosheets grown on Ni foam. Surfaces and Interfaces, 2018, 12, 102-107.	1.5	32
30	Direct growth of MnCO3 on Ni foil for a highly sensitive nonenzymatic glucose sensor. Journal of Alloys and Compounds, 2018, 762, 216-221.	2.8	14
31	Cu ₂ O templating strategy for the synthesis of octahedral Cu ₂ O@Mn(OH) ₂ core–shell hierarchical structures with a superior performance supercapacitor. Journal of Materials Chemistry A, 2018, 6, 13668-13675.	5.2	56
32	β-MnO2 microrods for the degradation of methyl orange under acid condition from aqueous solutions. Research on Chemical Intermediates, 2017, 43, 3975-3987.	1.3	8
33	Carbon spheres@MnO2 core-shell nanocomposites with enhanced dielectric properties for electromagnetic shielding. Scientific Reports, 2017, 7, 15841.	1.6	38
34	Combustion synthesized hierarchically porous Mn ₃ O ₄ for catalytic degradation of methyl orange. Canadian Journal of Chemical Engineering, 2017, 95, 643-647.	0.9	6
35	Enhanced microwave absorption properties of MnO2 hollow microspheres consisted of MnO2 nanoribbons synthesized by a facile hydrothermal method. Journal of Alloys and Compounds, 2016, 676, 224-230.	2.8	52
36	Facile synthesis of core–shell carbon nanotubes@MnOOH nanocomposites with remarkable dielectric loss and electromagnetic shielding properties. RSC Advances, 2016, 6, 90002-90009.	1.7	20

#	Article	IF	CITATIONS
37	Combustion synthesized hierarchically porous WO3 for selective acetone sensing. Materials Chemistry and Physics, 2016, 184, 155-161.	2.0	25
38	Self-grown MnO 2 nanosheets on carbon fiber paper as high-performance supercapacitors electrodes. Electrochimica Acta, 2016, 217, 16-23.	2.6	43
39	Effect of calcination temperatures on the electrochemical performances of nickel oxide/reduction graphene oxide (NiO/RGO) composites synthesized by hydrothermal method. Journal of Physics and Chemistry of Solids, 2016, 98, 209-219.	1.9	37
40	RGO/KMn8O16 composite as supercapacitor electrode with high specific capacitance. Ceramics International, 2016, 42, 5195-5202.	2.3	19
41	Binder-free NiO@MnO 2 core-shell electrode: Rod-like NiO core prepared through corrosion by oxalic acid and enhanced pseudocapacitance with sphere-like MnO 2 shell. Electrochimica Acta, 2016, 189, 83-92.	2.6	47
42	Reduced graphene oxide (RGO)/Mn3O4 nanocomposites for dielectric loss properties and electromagnetic interference shielding effectiveness at high frequency. Ceramics International, 2016, 42, 936-942.	2.3	70
43	Morphology control of porous CuO by surfactant using combustion method. Applied Surface Science, 2015, 349, 844-848.	3.1	47
44	A novel microwave absorption material of Ni doped cryptomelane type manganese oxides. Ceramics International, 2015, 41, 5688-5695.	2.3	16
45	Synthesis and photocatalytic degradation of methylene blue over p-n junction Co3O4/ZnO core/shell nanorods. Materials Chemistry and Physics, 2015, 155, 1-8.	2.0	68
46	A facile hydrothermal synthesis of MnO ₂ nanorod–reduced graphene oxide nanocomposites possessing excellent microwave absorption properties. RSC Advances, 2015, 5, 88979-88988.	1.7	113
47	Porous NiO nanosheets self-grown on alumina tube using a novel flash synthesis and their gas sensing properties. RSC Advances, 2015, 5, 4880-4885.	1.7	52
48	Hydrothermal synthesis of Co3O4 nanorods on nickel foil. Materials Letters, 2014, 123, 187-190.	1.3	22
49	Facile synthesis of α-MnO2 nanorods at low temperature and their microwave absorption properties. Materials Chemistry and Physics, 2014, 143, 1061-1068.	2.0	62
50	FACILE SYNTHESIS AND MICROWAVE ABSORPTION PROPERTIES OF $\hat{1}\pm$ -MnO2 NANORODS. Functional Materials Letters, 2012, 05, 1250043.	0.7	7
51	Frequency and temperature effects on dielectric and electrical characteristics of α-MnO2 nanorods. Powder Technology, 2012, 224, 356-359.	2.1	28
52	IN-SITU PREPARATION AND MAGNETIC PROPERTIES OF Fe ₃ O ₄ /WOOD COMPOSITE. , 2011, , .		1
53	Microwave absorption characteristics of manganese dioxide with different crystalline phase and nanostructures. Materials Chemistry and Physics, 2010, 124, 639-645.	2.0	53
54	Temperature dependent dielectric characterization of manganese dioxide nanostructures with different morphologies at low frequency. Journal of Alloys and Compounds, 2010, 507, 126-132.	2.8	20

#	Article	IF	CITATIONS
55	Effect of doping MnO2 on magnetic properties for M-type barium ferrite. Journal of Magnetism and Magnetic Materials, 2007, 311, 507-511.	1.0	36
56	Expanded Polystyrene as an Admixture in Cement-Based Composites for Electromagnetic Absorbing. Journal of Materials Engineering and Performance, 2007, 16, 68-72.	1.2	21
57	Investigation of the electromagnetic characteristics of cement based composites filled with EPS. Cement and Concrete Composites, 2007, 29, 49-54.	4.6	84
58	Cement based electromagnetic shielding and absorbing building materials. Cement and Concrete Composites, 2006, 28, 468-474.	4.6	231
59	Electromagnetic characteristics of nanometer manganese dioxide composite materials. Journal of Electronic Materials, 2006, 35, 892-896.	1.0	42
60	Effect of a coupling agent on the electromagnetic and mechanical properties of carbon black/acrylonitrile–butadiene–styrene composites. Journal of Applied Polymer Science, 2006, 102, 1839-1843.	1.3	9
61	A Discrete Slab Absorber: Absorption Efficiency and Theory Analysis. Journal of Composite Materials, 2006, 40, 1841-1851.	1.2	37